

A Prototype Tape System Using Multi Channel Stack Heads and Metal Evaporated Tape

Hiroaki Ono
Hiroaki.Ono@jp.sony.com
Masaaki Sekine
Masaaki.Sekine@jp.sony.com

Shinichi Fukuda
Shinichi.Fukuda@jp.sony.com
Tomoe Iwano
Tomoe.Iwano@jp.sony.com
Sony Corporation

Yusuke Tamakawa
Yusuke.Tamakawa@jp.sony.com
Seiichi Onodera
Seiichi.Onodera@jp.sony.com

Abstract

In magnetic recording systems, it has been reported that sufficient SNR was obtained with a narrow track width, using a spin-valve head and metal-evaporated tape. In order to apply this to a helical-scan tape system, techniques for writing narrow tracks and reading them exactly were required. However, the degree of mechanical accuracy demanded was too high to realize. With this in mind, we have developed multi-channel heads which can write and read certain tracks with a single scan, as well as a non-tracking technique removing the need for such precise mechanical accuracy. A prototype tape drive employing these techniques was developed, and a track density exceeding 15ktpi was achieved.

Also, we described here that improving the corrosion resistance of shielded spin valve (SV) head and ultra-thin metal-evaporated (ME) tape.

Index Terms—non-tracking, helical scan tape system, multi-channel stack head, spin-valve head, GMR head metal-evaporated tape, corrosion.

1. Introduction

It was reported at TMRC-2001 that areal-densities of 4.5Gbp² and 11.5Gbp² were achieved using two types of spin-valve heads and metal-evaporated tapes with a contact tape-head interface [1]. In case of 4.5Gbp², the report explained an SNR of 26dB was calculated based on a read head track width of 0.8 μ m.

Certain helical-scan tape format parameters [2]-[12] over the past 20 years are shown in Table 1. According to the table, even in the most recently established formats, the track pitches remained as wide as around 5 μ m. Therefore, the use of the spin-valve head can be expected to lead to a remarkable improvement in recording density.

However, the results of the above report were achieved by experiments using a spin stand tape tester, rather than a drive. If we try to record with this recording density using an actual tape drive, we have to develop techniques allowing the narrow tracks to be written, and a read head to scan the written track accurately.

In a helical scan tape system, there is a rotating drum in which the heads are mounted, and around which a tape is wrapped. Tracks are then written on the tape by heads scanned in a direction at a slanted angle from that of the running tape. The track pitch, angle and linearity are decided by mechanical accuracy, such as the fitting accuracy, and the stability of the drum rotation and tape operation. Therefore, if the track pitch narrows, a proportional reduction in mechanical errors will be necessary, although it is difficult to improve mechanical accuracy in the short term. In addition, during the reading process, considerable mechanical accuracy and a rapid servo technique are needed in order to trace the narrow track accurately.

Instead of solving these difficult points, we tried to create a narrow track system without improving mechanical accuracy. Therefore, we developed multi-channel stack heads and a non-azimuth non-tracking technique. Using these techniques, a prototype drive was made and a system with track density exceeding 15ktpi was achieved.

To apply spin-valve head and ultra-thin metal-evaporated tape are keys to obtain high recording density in tape system. However, archival reliability of them is concern.

We report here the development of corrosion-resistant spin-valve head and new lubricant for metal-evaporate tape. The storage life of spin-valve head and metal-evaporate tape were evaluated using the Battelle Class II test and estimated to be more than 10 years and 50 years respectively.

Table 1. Certain helical-scan tape drive parameters.

Format	DAT [2] DDS [3]	DDS2 [4]	DV [5]	DDS3 [6]	AIT-1 [7]	DDS4 [8]	AIT-2 [9]	VXA-1 [10]	MicroMV [11]	AIT-3 [12]	AIT-4	Prototype
λ (Nyquist)	0.666 μ m	0.666 μ m	0.500 μ m	0.333 μ m	0.350 μ m	0.333 μ m	0.243 μ m	0.365 μ m	0.286 μ m	0.291 μ m	0.22 μ m	0.240 μ m
Track Pitch (Tp)	13.6 μ m	9.1 μ m	10.0 μ m	9.1 μ m	11.0 μ m	6.8 μ m	11.0 μ m	9.1 μ m	5.0 μ m	5.5 μ m	4.4 μ m	1.6 μ m
Tp/ λ (Nyquist) Ratio	20	14	20	27	31	20	45	25	17	19	20	6.7
Recommended Equalize	Integer	Integer	PR4	PR1	PR1	PR1	PR1		PR4	EPR4	EPR4	PR4
Coding	8/10	8/10	24/25	8/10	8/10	8/10	16/20	(1,6) 8/14	24/27	16/18	16/18	24/27
Azimuth Angle	$\pm 20^\circ$	$\pm 20^\circ$	$\pm 20^\circ$	$\pm 20^\circ$	$\pm 25^\circ$	$\pm 20^\circ$	$\pm 25^\circ$	$\pm 20^\circ$	$\pm 25^\circ$	$\pm 25^\circ$	$\pm 25^\circ$	0°

Roughly sorted in chronological order

2. Read/Write performance using multi-channel stack heads

2.1. Multi-channel write head

The track accuracy was decided based on the mechanical accuracy because two adjacent tracks were written with different scans. Between the two scans, various mechanical errors or fluctuations occur, causing the written track width to vary. If several tracks can be written in a single scan, however, relations between them will not be dependent on mechanical accuracy. In order to achieve this, we developed a multi-channel stack write head. [13] [14]

Specification of the stack write head is shown in Table 2. Schematic view and microscopic image of the stack write head are shown in Figure 1. The four-channel write head was fabricated by stacking the four inductive heads using thin film photolithographic process. Each stacked head was designed as 3.5 μ m track width and shifted by 1.5 μ m.

The sketches of writing patterns using four-channel stack write head are shown in Figure 2. The width of the 1st to 3rd tracks does not depend on mechanical accuracy, but instead on that of the thin-film process. Since the latter has a level of accuracy superior to that of mechanical accuracy, narrow tracks can be written stably. However, the width of the 4th track is still depending on the mechanical accuracy, as in former systems. The standard width of the 4th track, however, is set up to be wider than the others so that it is guaranteed at least equivalent width; even if its own width narrows due to mechanical fluctuations.

Table 2. Specifications of 4channel stack write head.

Four-channel write head	
Number of channels	4
Track width	3.5 μ m
Coil	7turn
Recording gap	0.15 μ m

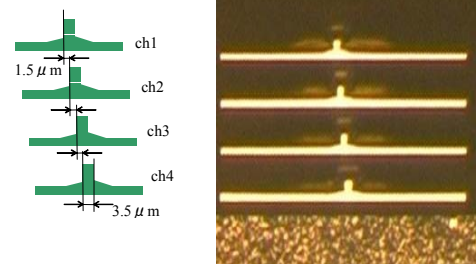


Figure 1. Schematic view and microscopic image of 4channel stack write head.

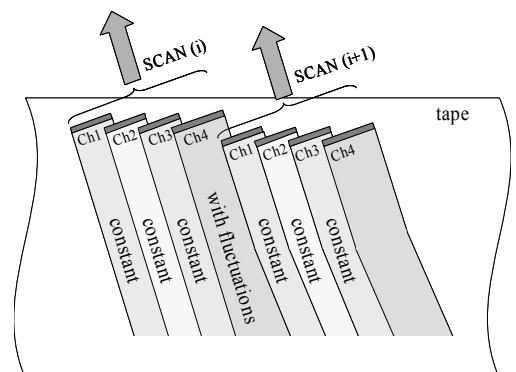


Figure 2. Writing patterns using 4channel stack write head.

The Magnetic force microscope (MFM) image of recorded patterns using four-channel stack write head is shown in Figure 3. Different frequencies were used for each channel in this observation. Each track pattern is over-written by adjacent head, which boundaries are defined as the track width without a guard band. It is also confirmed that each write head indicated almost same saturation characteristics as shown in Figure 4.

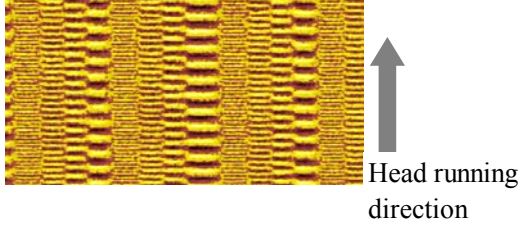


Figure 3. MFM image of writing track patterns using 4channel stack head.

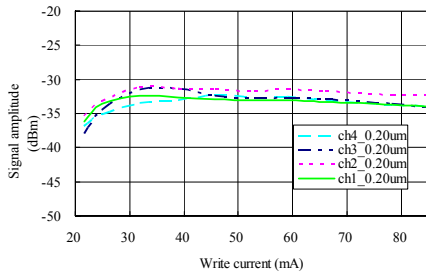


Figure 4. Saturation characteristic of multi-channel write head.

2.2. Limitation of azimuth recording

An azimuth recording without a guard band between tracks, as shown in Figure 5, was used in the helical-scan tape system. In azimuth recording systems, the read head width is set up to be wider than the written track pitch, hence the ability of the read head to scan the full width of a track. Although the read head scans adjacent tracks too, the signals from adjacent tracks decreased owing to the effect of azimuth loss.

When the ratio of the reading signal level from one adjacent track to that of the home track is set to E , E is expressed by expression (1), as follows:

$$E = \frac{Wa}{Wh} \cdot \frac{\sin \frac{\pi G \cos 2\theta}{\lambda \cos \theta}}{\sin \frac{\pi G}{\lambda \cos \theta}} \cdot \frac{\sin \frac{2\pi Wa \tan \theta}{\lambda}}{\frac{2\pi Wa \tan \theta}{\lambda}} \quad (1)$$

Where, Wh is the home track width, Wa the scanning width on one adjacent track, G the head gap length, θ the azimuth angle and λ the wavelength.

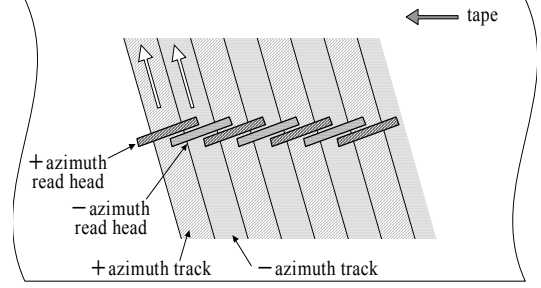


Figure 5. Azimuth track pattern and on-track reading.

A signal to crosstalk noise ratio, abbreviated as SXR, calculated on a channel using a partial response class 4 (PR4) and 24/27 coding [15] is shown in Figure 6. This was calculated by integrating expression (1) with respect to frequency. The S of the SXR is an eye-pattern height of the desired signal from the home track, and the X is the undesired signal rms level from both of the adjacent tracks. The frequency is equivalent to the relative speed between a head and a tape divided by λ .

It is clear that as the track pitch narrows, the SXR deteriorates. However, to effectively exploit the high output sensitivity of the spin-valve head, the track pitch must be narrowed, meaning we cannot count on the azimuth effect. Moreover, because the application of an azimuth angle to the thin-film multi-channel head is problematic, we decided to abandon the azimuth recording technique previously used for years.

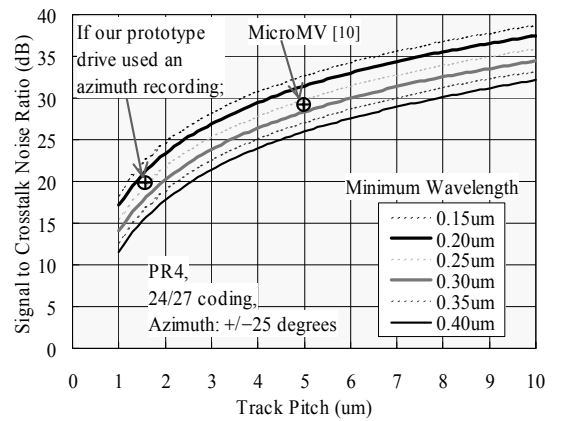


Figure 6. Signal to crosstalk noise ratio.

2.3. Non-azimuth, non-tracking technique.

A read head is frequently controlled to trace on just a single written track. However, in a few helical-scan systems a non-tracking technique has been employed [10] [11] [16] [17]. Normally, in non-tracking systems, the read scanning density is double, namely, two scans for a single written track. Figure 7 explains the non-tracking aspect of azimuth recording.

The read head width is set to be almost double the track pitch, so that a written track can be fully covered with at least one of two reading scans at every tracking phases of reading scans. The tracking phase is defined so that the same-azimuth track pitch corresponds to 360 degrees.

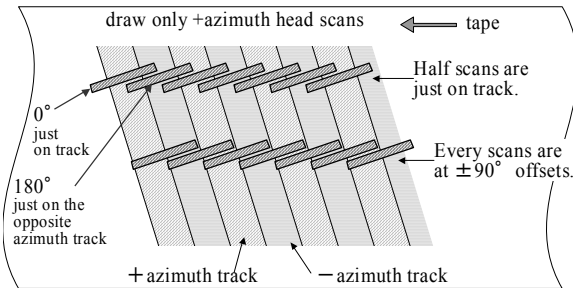


Figure 7. Non-tracking in azimuth recording.

The signal in a track consists of many blocks, each of which can be detected independently and meaning a track need not be read back in one continuous scan. If a block is detected twice by different scans, the block with fewer errors is employed. With in this mind, it does not matter whether the angle of a reading scan differs from that of a written track. The advantage of the non-tracking system is that it eliminates the necessity for mechanical accuracy concerning the scanning angle or written track linearity.

We move on now to the non-tracking techniques for non-azimuth recordings. Generally the read head width in non-azimuth recording should be set narrower than the written track pitch, to avoid any signal from adjacent tracks being read.

In a non-azimuth, non-tracking system (abbreviated to NANT), the track width of the read head should be less than half the written track pitch. Therefore, as shown in Figure8, at least half of the read scans will be capable of reading single tracks without straddling the adjacent tracks.

The NANT system includes the advantage of eliminating the need for accuracy of the head scan angle or linearity, just as in the non-tracking system in azimuth recording. However, a stable scanning pitch is needed. If a scanning pitch happens to be wide, the written track

between the two scans will not be readable without straddling adjacent tracks in each scan. Since this scanning pitch accuracy was difficult to obtain as a factor of overall mechanical accuracy; hence we developed a multi-channel read head to fix the scanning pitch through the thin-film accuracy process.

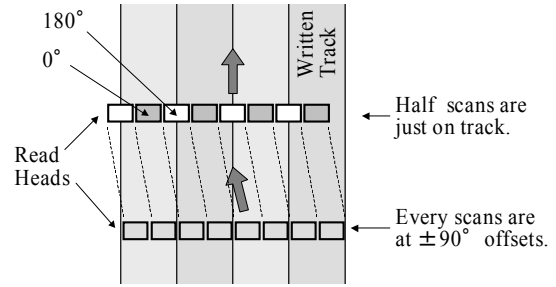


Figure 8. Non-tracking in non-azimuth recording.

Specification of the stack read head is shown in Table3. Schematic view and microscopic image of the stack read head are shown in Figure 9. The eight-channel read head was fabricated by stacking the four layers consists of two spin valve elements in one layer as shown in Figure 9. Read track-pitch was designed with 0.75um at half of write track-pitch, because one of adjacent two heads can always read a recorded track.

Table 3. Specification of 8channel stack read head

Eight-channel GMR head	
Number of channels	8
Track width	0.75um
MR height	0.6um
Shield to shield distance	0.18um

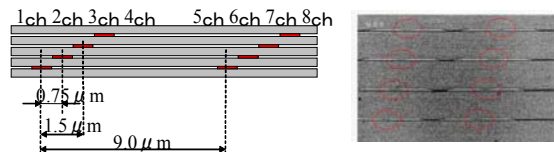


Figure 9. Schematic view and microscopic image of 8ch stack read head.

Although scanning pitches between multiple channels in a single head are decided based on thin-film accuracy, the scanning pitch between two scans is still a factor of mechanical accuracy. One of the solutions involves the scanning pitch is being adjusted to partly overlap the

previous scan. This overlap width is determined taking the mechanical fluctuation width during a single scanning interval into consideration.

2.4. Influence of mechanical error

The influence of mechanical error can be reduced using multi-channel heads and NANT techniques. However, as the track pitch narrows, the influence of mechanical errors must be considered on a quantitative basis. The most sensitive case involves the read heads scanning twice onto one track, the 90 degrees case in Figure 8, because the read heads can then shift onto adjacent tracks easily if the track width becomes narrow, or the interval between the read heads spreads or the read head width becomes wider. We used simulations to consider such situations.

The results are described below. A track profile model of the read head sensitivity is defined as shown in Figure 10. The track profile of Figure 10 was surmised based on the actual profiles of the spin-valve heads. An effective read-head width (Wh) is defined as a track width from which more than half the sensitivity of the overall track center sensitivity was obtainable.

Figure 11 shows the written magnetic levels on the tape around the boundary of two tracks. These curves were modeled based on the actual tape patterns, which were measured by a magnetic force microscope (MFM) and analyzed with the fundamental waveform levels.

Four parameters were introduced, namely the signal to noise ratio (SNR) in the case of center tracking, the written track width (Ww), the read head scanning pitch (Wr), and the read head width (Wh). Under standard conditions, Ww is $1.5\mu\text{m}$ and Wr is $0.75\mu\text{m}$.

The off-track characteristics of the block error rate in the case of an SNR of 17dB and Ww of $1.5\mu\text{m}$ are shown as thin lines like bathtub curves in Figure 12. As the read head goes further from the track center, the error rate worsens. However, the next read head then comes to scan the track from the opposite side to compensate for the error rate. In such cases, a track is scanned twice by the read heads, causing the error rate to become equivalent to the product of two error rates, if errors are caused by random noise. Therefore, the error rates in NANT become the curves shown as bold lines in Figure 12.

The worst and average off-track error rates respectively were evaluated from the bold curves in Figure 12 as a function of Ww , Wr and Wh . For the read head, the decrease in Ww , increase in Wr and increase in Wh had virtually the same influence on the quantity of adjacent track reading. This meant the variables, ΔWw , ΔWr and ΔWh , were summarized to ΔEa as follows,

$$\Delta Ea = \Delta Ww + \Delta Wr + \Delta Wh \quad (2)$$

Where, ΔWw , ΔWr and ΔWh are defined as follows, using $Ww0$, $Wr0$ and $Wh0$, as the standard widths of Ww , Wr and Wh respectively;

$$\Delta Ww = Ww0 - Ww, \quad (3)$$

$$\Delta Wr = Wr - Wr0, \quad (4)$$

$$\Delta Wh = Wh - Wh0, \quad (5)$$

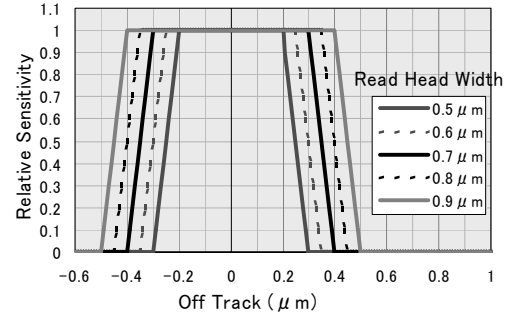


Figure 10. Sensitivity model of read head.

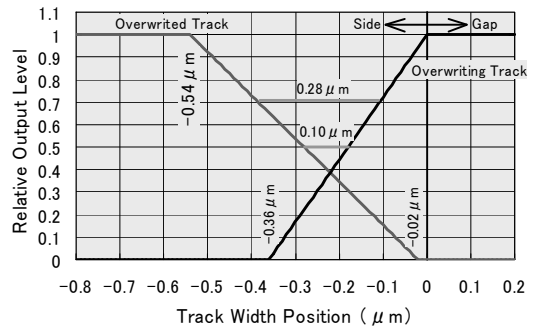


Figure 11. Output Level at Tape Edges.

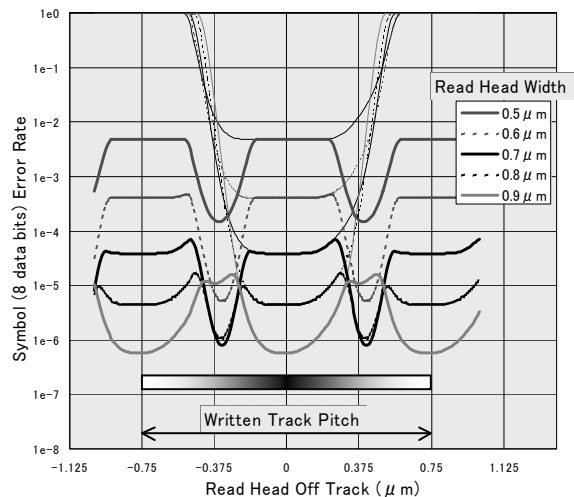


Figure 12. NANT error rate off-track characteristics.

In our simulations, $Ww0$ equals $1.5\mu\text{m}$ and $Wr0$ equals $0.75\mu\text{m}$. ΔEa is called “track error” as shown in Figure13.

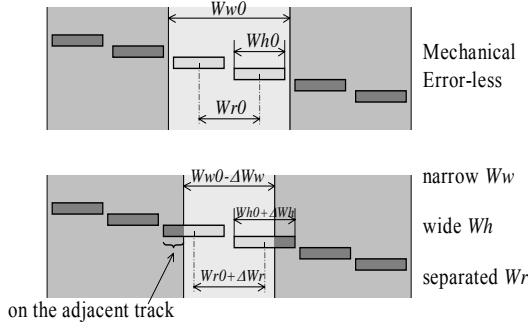


Figure 13. “Track Error” is defined as the sum of ΔWw , ΔWr and ΔWh .

The worst error rate as a function of track error at an SNR of 18dB is shown in Figure 14. We can see in Figure14 that in order to guarantee the worst error rate of $1e-3$, we have to limit the track error to within $0.2\mu\text{m}$. In systems with an SNR of 18dB, the level of track error will be a standard for thin-film process accuracy.

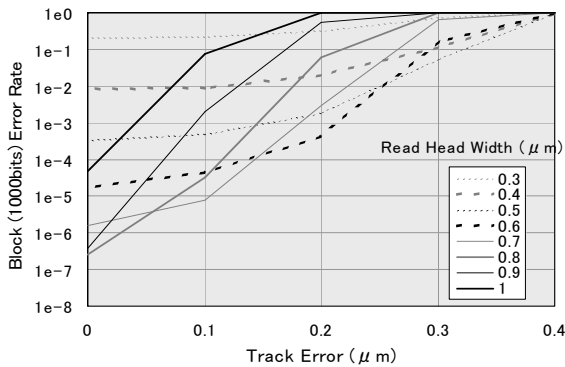


Figure 14. Worst error-rate track-error at an SNR of 18dB

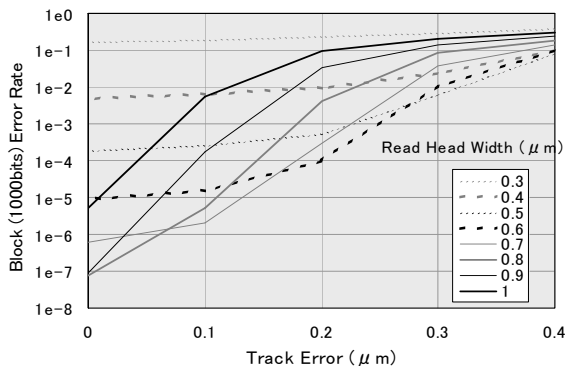


Figure 15. Average error-rate track-error at an SNR of 18dB.

Figure15 shows the average error rate. When an error correction code with a long interleave extending to many tracks is usable, the average rather than the worst error rate may be a better choice to evaluate the system, because the worst scanned track can be compensated for by nearby tracks through error correction.

Figure 16 and 17 show the worst and average error rates respectively at an SNR of 20dB. We can see in Figure16 that for the worst error rate of $1e-3$, we have to limit the track error to within $0.3\mu\text{m}$.

It is clear that when the SNR becomes good, the maximum permissible dose of track error will increase. This let us design the helical scan tape drive balancing the SNR and the level of track error.

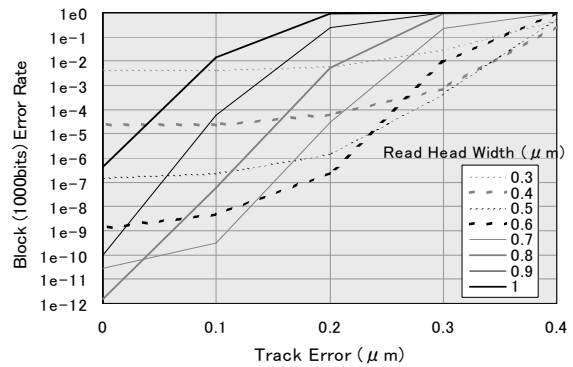


Figure 16. Worst Error-rate Track-error at an SNR of 20dB.

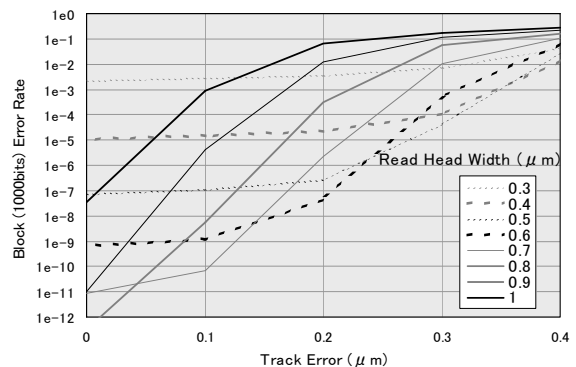


Figure 17. Average Error-rate Track-error at an SNR of 20dB.

2.5. A Prototype drive

We have developed a prototype drive whose principal specifications are shown in Table 4. The drive has a write head with 4 channels and a read head with 8 channels. The track width of the 4th channel is set to 2 μ m, namely 0.5 μ m wider than that of channels 1 to 3 as a margin for mechanical error or fluctuations.

Table 4. Specifications of the prototype drive.

Drum Diameter	40mm
Track Width of Ch1 to Ch3	1.5 μ m
Track Width of Ch4	2.0 μ m
Tape Width	8mm
Write Channel	4ch
Read Channel	8ch
Coding Rate	8/9
Channel	PR4ML
Write Data Transfer Rate	20MBps
Channel Clock	148MHz
Minimum Wavelength	0.240 μ m
Linear Density	188kbp
Track Density	15.6ktp
Areal Density	2.94Gbp ²

The read channel block diagram is shown in Figure 18. As an error correction code, the two-dimensional Reed-Solomon code was employed. The read signal is detected and checked the inner ECC code (C1) of each block in each channel. Subsequently, the blocks are constructed in an NT processing circuit based on the address information of each detected block. The outer code (C2) has a uniform Latin square interleaving [18] extended to 32 tracks, while the outer code has redundancy of 25%, allowing quarter of the tracks to be corrected.

Figure 19 shows the beginning of the written track pattern. The written wavelength was 0.48 μ m for channels 1 and 3, and 1.2 μ m for channels 2 and 4. In Figure 19, channels 1 and 3 appear as bright lines, and channels 2 and 4 as dark lines. Although track width fluctuations are

apparent in channel 4, the minimum width of the latter is wider than that of channel 2, which looks as dark as channel 4.

In order to observe the state of the NANT reading, we analyzed which read-head read which written track, of which an example is shown in Figure 20. Four channels of written tracks are drawn with different degrees of shading; clearly indicating that the track is composed of data on several read channels.

This drive can transfer the data to a PC bi-directionally via a USB interface. We recorded a file from the PC onto a tape, then reconstructed it from the tape to the PC, and confirmed that the reconstructed file was the same as the original. The writing data transfer rate was 20MBps (160Mbps).

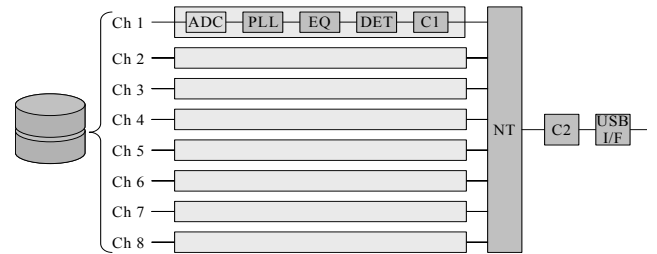


Figure 18. Read channel block diagram.

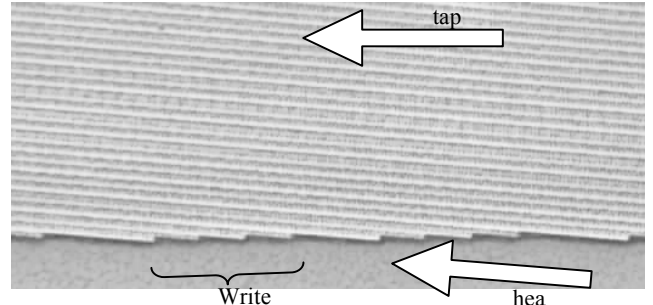


Figure 19. Beginning of the track.

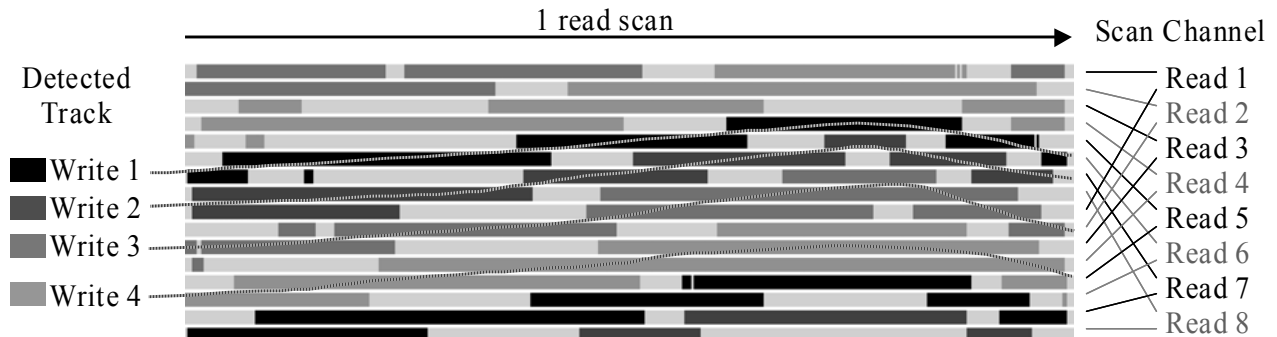


Figure 20. Track is composed of several read heads.

3. Reliability of spin-valve head and metal evaporate tape

3.1. Corrosion-resistant spin-valve head

The head surface in the tape system is subject to wear without a protective coating, therefore the spin-valve (SV) sensor of the GMR head suffers corrosion environment. We developed a corrosion-resistant spin valve element in this point of view [19].

The corrosion-resistant spin-valve element (Ta/NiFe/CoNiFe/CuAu/CoNiFe/PtMn/Ta) composed of a CuAu layer and a CoNiFe layer instead of the Cu layer and CoFe layer of conventional spin-valve element (Ta/NiFe/CoFe/Cu/CoFe/PtMn/Ta).

A corrosion-resistant GMR head using a corrosion-resistant spin-valve element was fabricated. The head surface on the spin-valve element had no protective coating such as diamond-like carbon (DLC). The Battelle Class II test was used to evaluate the corrosion resistance. In this test, the temperature and relative humidity are 30°C and 70%, respectively. The concentrations, in parts per billion, of H₂S, Cl₂, and NO₂ gases are 10, 10, and 200, respectively.

Figure 21 shows the transfer curves of the GMR head before and after the Battelle Class II test for 20 days, which corresponds to the environmental pollution a PC will experience in 10 years. The transfer curves did not change after the test. Therefore it is estimated that the corrosion-resistant GMR head maintains its magnetic properties more than 10 years.

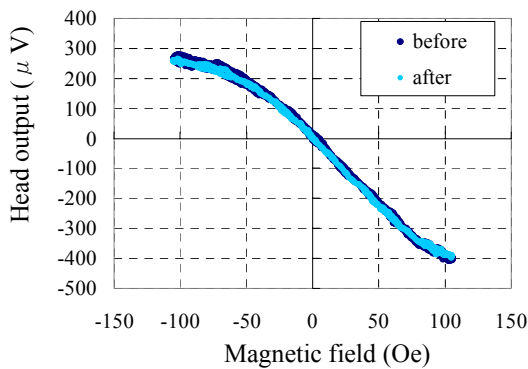


Figure 21. Transfer curves before and after gas test. (Battelle Class II test for 20 days)

3.2. Improving the corrosion-resistance of ultra-thin metal evaporate tape

In order to obtain high recording density, magnetic layer thickness of metal evaporated (ME) tape must be thinner than that of conventional ME tapes. For example, 4.5Gbp₂ and 11.5Gbp₂ were achieved using less than 33nm thick magnetic layer [20]. We developed a new lubricant with carboxyl groups, which can improve corrosion resistance of ultra-thin ME tapes.

ME tape with 33nm thick Co-O ferromagnetic film, coated by diamond-like carbon (DLC), was used in this test. Its structure is shown in Figure 22.

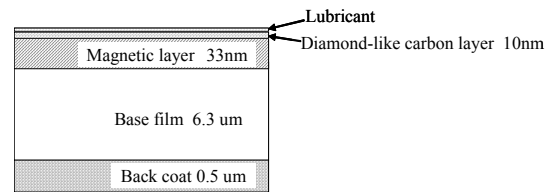


Figure22. A schematic cross sectional view of the ME tape.

Three lubricants A (with no carboxyl group), B (with one carboxyl group), and C (with two carboxyl groups) were synthesized. Lubricant with more than three carboxyl group has too small solubility to make uniform layer. Each lubricant has the same perfluoro-alkyl chain as hydrophobic group, and the molecular weight is between 500 and 1000.

Each lubricant was applied in turn to the DLC. The amount of lubricant on the ME tape surface was measured using X-ray Photoelectron Spectroscopy (XPS) and the amount of isopropyl alcohol extracted lubricant from ME tape was measured using Liquid Chromatography Mass Spectroscopy (LC/MS). The XPS data was converted to physical quantity using LC/MS data.

The test specimens are shown in Table 5, and the amount of remaining lubricant on DLC after extract process is shown in Table 6. The remaining lubricant indicates the amount of lubricant that is bonded to DLC.

The Battelle Class II test was also used to evaluate the corrosion resistance. Each tape sample was exposed for 10 days.

To quantify corrosion damage, samples after the test were evaluated using demagnetization ratio X, which is defined as $X(\%) = \Delta M \times 100 / M_{ini}$, $\Delta M = M_{ini} - M$, where M is the ME tape magnetization which is measured using a Vibrating Sample Magnetometer (VSM) and M_{ini} is the initial value of M [21].

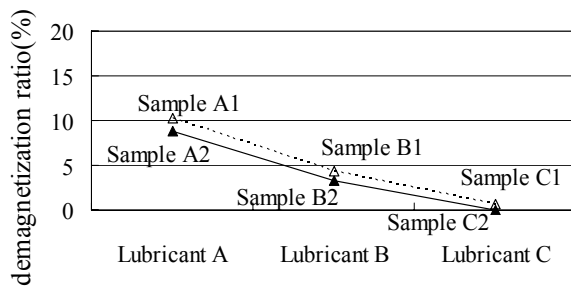
Table 5. Test specimens.

Sample	Lubricant	Amount of lubricant on DLC layer (mg/m ²)
A1	A	1.3
B1	B	1.3
C1	C	1.3
A2	A	2.9
B2	B	2.9
C2	C	2.9

Table 6. Amount of remaining lubricant.

Sample	Amount of remaining lubricant on DLC layer (mg/m ²)
A1	0.14
B1	0.21
C1	0.31

Figure 23 shows the demagnetization ratio of each sample after the Battelle Class II test. When the magnetic layer is corroded, the demagnetization ratio increases. The amount of lubricant affects the corrosion resistance; however the number of carboxyl groups is more effective in reducing the demagnetization ratio. This suggests that lubricant C with one molecule with two carboxyl groups is more effective than lubricants A and B with two molecules and with no carboxyl group and with one carboxyl group, respectively. This also suggests that the adsorptivity of the lubricant is more effective than the amount of lubricant.

**Figure 23. Demagnetization of ME tape dependence on the number of carboxyl groups and the amount of lubricant after 10 days of Battelle Class II test.**

The corrosion mechanism of magnetic media with a DLC layer was reported to start from a pinhole in the DLC layer in an environment that includes H₂O, O₂, and ionic contaminants such as chlorides or sulfates [22]. When the lubricants have the same hydrophobic group, the water-repellent property of the surface is influenced by the amount of lubricant rather than the functional group. This indicates that Lubricant C may have a small effect on repelling H₂O that includes ionic contaminants, however the new lubricant can prevent corrosion reaction by bonding to DLC.

To confirm the archival reliability of ME tape after the Battelle Class II test, Samples A and C were set in an AIT-cartridge and exposed to a Battelle Class II environment for 100 days, which is equivalent to 50 years in a commercial computer facility [23].

The block error rate in a helical-scan tape drive system were measured using a modified AIT-2 drive, whose reading head was changed from an inductive head to an anisotropic magneto-resistive (AMR) head.

Figure 24 shows the images of Samples A1 and C1 under the lid of a cartridge after 100 days of a Battelle Class II test. In an AIT cartridge, the lid corrodes more easily than other places as 8mm video cassette [24]. However there is little corrosion on Sample C1, although considerable corrosion is observed on Sample A1.

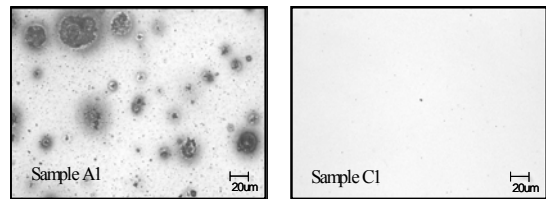
**Figure 24. Surface image of Sample A1 and C1 under the lid after 100 days of Battelle Class II test.**

Figure 25 shows the block error rate of Sample C1 after 100 days exposure in a Battelle Class II test environment. The linear recording density is 212k FRPI, and the read-head width is 7.5µm. The error rate is stable even after 100 days of the Battelle Class II test. From this result, it can be seen that Sample C1 can be applied to commercial use even after 100 days of a Battelle Class II test, and we estimate that the storage life of ME tape with dicarboxy acid as a lubricant is more than 50 years.

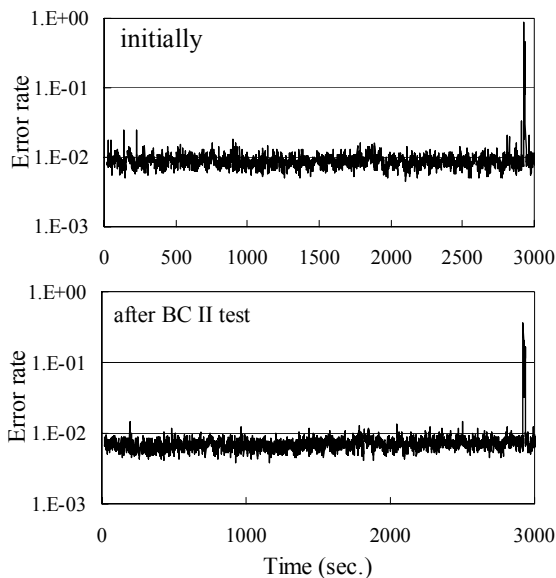


Figure 25. Error rates of sample C1 before and after 100 days of Battelle Class II test. Elevations of error rate at 2930 second of both measurements are due to a defect in the tape.

4. Conclusion

We developed multi-channel stack heads and a non-tracking, non-azimuth (NANT) technique to achieve a helical-scan tape drive with a narrow track pitch to effectively utilize the high sensitivity of the spin-valve head. This simulation showed that this system could be implemented, while a prototype drive with a minimum track pitch of 1.5 μ m was developed. Using this drive, we achieved data transfer to/from the PC at a user-data writing-rate of 20MBps.

The prototype drive proved that the multi-channel stack heads and NANT technique were applicable to a narrow-track helical-scan tape-system. The transfer rate would be increased by using more heads, more multi-channels per head or a higher channel clock frequency.

We developed a corrosion-resistant spin-valve element which composed of a CuAu layer and a CoNiFe layer instead of the Cu layer and CoFe layer of conventional spin-valve element. The magnetic properties of the corrosion-resistant spin-valve head are estimated to last for ten years in a commercial computer facility.

We also developed new lubricant with two carboxyl groups for ultra-thin metal evaporated tapes. The evaluated storage life of the ultra-thin ME tape with the developed lubricant is more than 50 years.

5. Acknowledgment

The authors would like to thank the members of the ATS Development Dept., Sony Corp. for developing the prototype drive, the members of CT Development Group, Sony Corp. for developing the channel methods and circuits for LSI, and MR Device Div., Sony Corp. for developing the multi-channel stack heads.

6. REFERENCES

- [1] T. Ozue, M. Kondo, Y. Soda, S. Fukuda, S. Onodera and T. Kawana, "11.5-Gb/in² Recording Using Spin-Valve Heads in Tape System", IEEE Trans. on Mag., VOL. 38, NO. 1, pp. 136-140, January 2002.
- [2] ISO/IEC61119, 1992.
- [3] Standard ECMA-139, 1990.
- [4] Standard ECMA-198, 1995.
- [5] ISO/IEC61834, 2001.
- [6] Standard ECMA-236, 1996.
- [7] Standard ECMA-246, 1996.
- [8] Standard ECMA-288, 1999.
- [9] Standard ECMA-292, 1999.
- [10] Standard ECMA-316, 2001.
- [11] K. Tsuneki, Y. Kotani, K. Iesaka, M. Mizuno, N. Kondo, Y. Yanagi, Y. Aoki, T. Himeno and Y. Senshu, "Development of a High-Density Magnetic Recording System for a Consumer VCR Using an MR Head", IEEE Trans. on Mag., vol. 38, no. 5, pp. 2274-2276, September 2002.
- [12] Standard ECMA-329, 2001.
- [13] T. Ozue, M. Kondo, K. Suzuki, S. Terui and T. Shibata, "Adjacent Multi-channel Head in Helical-scan Tape Systems", in Digest of Intermag, Boston, MA, USA, 2003, DQ-09.
- [14] T. Ozue, "Multi-track Recording in Helical-scan Tape Systems", in INSIC 2003, Alternative Storage Technologies Symposium, Monterey, CA, USA, June, 2003..
- [15] M. Noda, "A High-Rate Matched Spectral Null Code", IEEE Trans. on Mag., VOL. 34, NO. 4, pp. 1946-1948, July 1998.
- [16] T. Fukami, S. Fukuda, K. Maruyama, H. Ino and K. Odaka, "A New Play-back Method for R-DAT Using "Non-Tracking" Signal Processing", IEEE Trans. on Consumer Electronics, Vol. 37, No. 4, pp. 814-822, November, 1991.
- [17] T. Himeno and T. Katoku, "High-density Magnetic Tape Recording by Non-tracking Method", IEEE Journal of Magnetism and Magnetic Materials 134, pp. 255-261, 1994.
- [18] K. Kondou and M. Noda, "Uniform Latin Square Interleaving for Correcting Two-dimensional Burst Errors", IEEE Intermag 2005 Digests, pp. 498 (EP10), April 2005.
- [19] H. Tetsukawa, "Spin-Valve Head With Corrosion Resistance for Tape Recording System", IEEE Trans. Magn., vol. 40, No. 6, pp. 3541-3544, 2004.
- [20] H. Tetsukawa, M. Kondo, Y. Soda, T. Ozue, K. Motohashi, S. Onodera and T. Kawana, "Recording characteristics on thin metal evaporated media in a helical-

scan tape system with a spin-valve head”, IEEE Trans. Magn., vol. 38, pp1910, 2002.

- [21] T. Kawana, T. Takeda, T. Uchimi and K. Sato, “Archival stability of metal evaporated tape”, J. Magn. and Magn. Mater., vol.155, p273, 1996.
- [22] J. Ying, T. Anokin and C. Martner, “Evolution of the corrosion process on thin-film media”, J. Vac. Sci. Technol. A, vol. 18, p1804, 2000
- [23] A. Djalali, D. Seng, W. Glatfelter, H. Lambropoulos, J. S. Judge and D.E. Speliotis, “Study of the stability of metal particle data recording tapes”, J. Electrochem. Soc. Vol. 138, p2504, 1991
- [24] H. Yoshida, H. Ouhata, Y. Nishizawa, K. Hibino and N. Satou, “Reliability of ME tape with DLC film in the field test”, (In Japanese), Technical Report of IEICE. MR95-33,1995